Molecular Dipole Chains III: Energy Transfer

J. J. de Jonge,[†] M. A. Ratner,*[,†] S. W. de Leeuw,[‡] and R. O. Simonis[‡]

Department of Chemistry, Northwestern University, Evanston, Illinois 60208, and Physical Chemistry and Molecular Thermodynamics, DelftChemTech, Delft University of Technology, Julianalaan 136, 2628 BL, Delft, The Netherlands

Received: August 26, 2003

Energy transfer in initially excited dipole chains was studied using simple one-dimensional models. Two types of chains were studied: the altitudinal dipole chain, in which all the dipoles rotate around the same axis, and the azimuthal dipole chain, in which the chain axis lies in the rotation planes of the dipoles. The analytic treatment of a pair of dipoles shows that energy transfer from dipole to dipole can only be complete for low excitations. At higher excitations, the excited dipole rotates too quickly for the second one to follow. Molecular dynamics simulations of 25-dipole chains show that energy transfer is possible in these chains. In some limiting cases, the energy transfer shows a soliton-like behavior. The altitudinal chain shows such behavior for low excitations, but for high excitations the rest of the chain cannot follow the excited dipole. In the azimuthal chain, the soliton-like behavior is more difficult to find: Both for low and high excitations the system shows no noticeable energy transfer. Only for certain excitations with intermediate energy can a soliton-like transfer be observed.

1. Introduction

By means of feedback controlled lithography[1] it is now possible to fabricate planar structures in which molecules are placed at specific points on a surface. Hence, individual arrangements of molecules can be placed on surfaces with arbitrary spacings and relative geometries. Such arrays may provide entirely new approaches to signal processing, sensing, and energy modulation, all based on rotational motions in molecular adlayers. Such structures extend the considerations that have been previously advanced for discussing rotational excitations in quasi one-dimensional stacked materials, including stacked phthalocyanine crystals (where they modulate the electron-transfer process along the chain[2]), and charge transport along columnar stacks of triphenylene dimers.[3] They also relate to the study of rotational excitations in rotator phase crystals[4] and, more generally, in molecular crystals.

The current paper addresses the simplest situation, namely finite, periodic one-dimensional strands. Two situations may occur: Figures 1a and 1b show the difference between so-called altitudinal rotor array, in which the planes of rotation are stacked above one another in an arrangement reminiscent of phthalocyanine stacks,[5] and the azimuthal array, in which the rotations occur in the plane of the intermolecular axis. Both these structures are attainable by lithographic deposition techniques on surfaces.

Previous analytical and simulation work[6−8] has addressed the low energy behavior, dispersion relations, group velocities and some aspects of energy transfer in both the altitudinal and the azimuthal chains. Rozenbaum[6,9] has published extensively on one- and two-dimensional arrays of interacting molecular rotors. While these studies, and the current work, are limited to Hamiltonian systems, Michl and his collaborators[11] have also considered situations in which the rotor molecules encounter frictional forces, as well as driving terms.

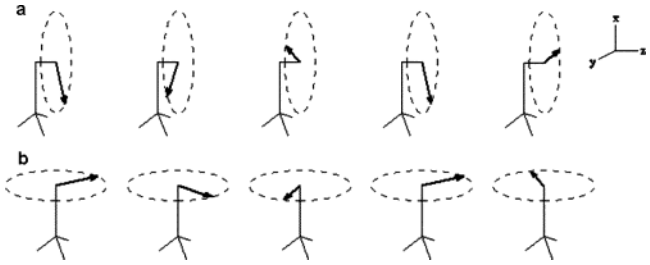

Figure 1. Chains of (a) altitudinal dipoles and (b) azimuthal dipoles mounted on a surface. The altitudinal dipoles are rotating in planes perpendicular to the surface, whereas the azimuthal dipoles rotate in the same plane containing the rotation axis.

This paper begins with formal analysis of the coupled dimer, for which analytical results are obtainable. For the altitudinal rotors, the angular momentum is a constant of the motion, so that only the relative angle of the two rotors is significant. As a function of the initial excitation, there is a low energy regime in which energy transfer from one rotor to the other is quite complete; above a critical energy, however, the energy transfer is negligible, because of inertial effects. In the azimuthal array, angular momentum is no longer conserved (spatial invariance is no longer present), and both angles are relevant for discussing excitations. There are now two critical points; above the higher one, energy transfer is once again essentially negligible.

Rotational energy transfer and excitation motion in finite chains of azimuthal and altitudinal rotors were investigated by molecular dynamics simulations. The critical points that were found for the pair are close to those found for the extended systems, although no analytical solution is possible for the latter systems. Pulse-like or soliton-like[10] excitations can be observed, and a striking cutoff behavior, which might find application as a high excitation filter, was found.

* Corresponding author.
[†] Northwestern University.
[‡] Delft University of Technology.

10.1021/jp0365458 CCC: $27.50
Published on Web 02/03/2004

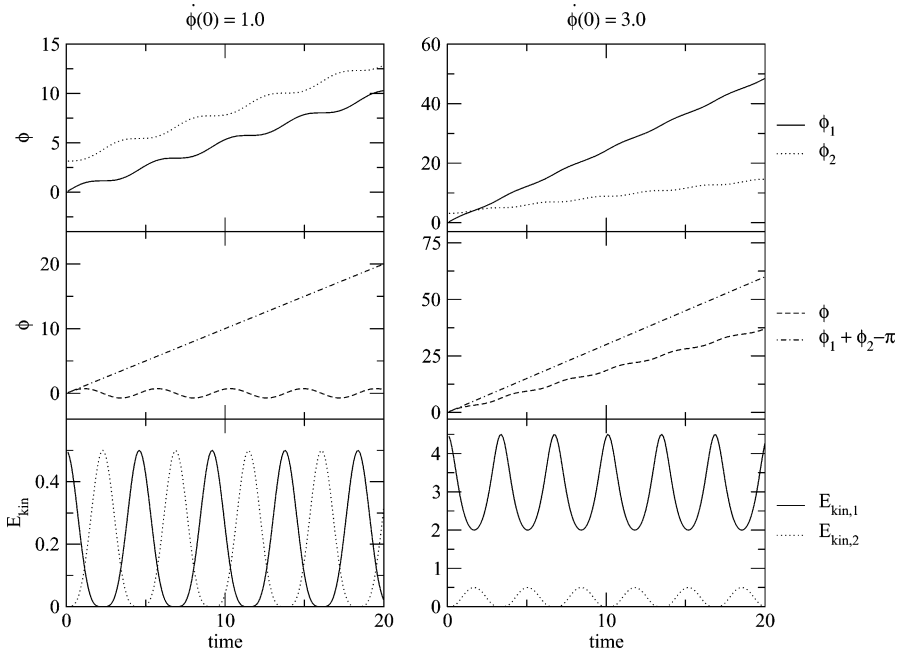

Figure 2. Angles and kinetic energies for an altitudinal dimer system in which the initial conditions lead to an oscillation (left) or increase (right) of the difference angle $\phi_1 - \phi_2$. Reduced units are used (see Appendix), $I_i = 1$, $\mu_i = 1$, $r_{ij} = 1$ such that $\omega_0^2 = 1$.

Starting from a Lagrangian, the equations of motion are derived in section II. Section III describes the analytical solutions for both dimers. The results of molecular dynamics simulations of 25-dipole chains are described and discussed in section IV.

The major focus of the current manuscript is on energy transfer in finite perfect chains. If one allows for friction effects, impurities, branching chains, and different initial conditions, the behavior of these rotor assembles is almost certain to be more varied. Future publications will address those issues.

2. Lagrangian and Equations of Motion

We consider antiferromagnetic point dipoles, which can rotate in a plane around their center of mass. The positions of the centers of the dipoles are fixed. The dipoles are only allowed to rotate in a plane, and their magnitudes do not change in time. The motion of the dipoles can be written in terms of a rotational angle ϕ_i.

Using the Euler−Lagrange equations one can find the equations of motion for ϕ_i:

$$\frac{\mathrm{d}}{\mathrm{d}t}\left(\frac{\partial L}{\partial \dot{\phi}_i}\right) = \frac{\partial L}{\partial \phi_i} \tag{1}$$

in which L is the Lagrangian of the system. For N dipoles it can be written in terms of $\vec{\mu}_i$ as

$$L = \sum_{i=1}^{N} \frac{I_i}{2\mu_i^2}\dot{\vec{\mu}}_i^2 - \sum_{i=1}^{N-1}\sum_{j=i+1}^{N}\left[\frac{\vec{\mu}_i\cdot\vec{\mu}_j}{r_{ij}^3} - 3\frac{(\vec{\mu}_i\cdot\vec{r}_{ij})(\vec{\mu}_j\cdot\vec{r}_{ij})}{r_{ij}^5}\right] \tag{2}$$

Here, I_i, $\vec{\mu}_i$, and $\vec{r}_{ij}$ are the moment of inertia of the ith dipole, its dipole moment, and the distance vector between dipoles i and j, respectively. In different spatial arrangements of the dipoles, the potential energy depends in different ways on the orientation angles ϕ_i of the dipoles.

In this paper we consider only two geometrical configurations. Both are equidistant linear arrays (chains) of dipoles, but with different rotational constraints imposed on the dipoles. In one case the dipoles are assumed to be mounted on a surface, such that the plane of rotation is perpendicular to that surface, the altitudinal rotor (Figure 1a). In the altitudinal chain all the dipoles rotate around the same axis. In the other case the dipoles are assumed to be mounted on the surface such that they rotate in a plane parallel to that surface: the azimuthal dipole rotor (see Figure 1b).

In these situations, the Lagrangian given by eq 2 becomes considerably simpler. For the altitudinal dipole chain (Figure 1a) the dipole moments $\vec{\mu}_i = \mu_i(\cos\phi_i, \sin\phi_i, 0)$ are always perpendicular to the center to center distance vectors $\vec{r}_{ij} = (0, 0, r_{ij})$. In this case eq 2 becomes

$$L = \sum_{i=1}^{N}\frac{I_i}{2}\dot{\phi}_i^2 - \sum_{i=1}^{N-1}\sum_{j=i+1}^{N}\frac{\mu_i\mu_j}{r_{ij}^3}\cos(\phi_i - \phi_j) \tag{3}$$

Using the Euler−Lagrange equation (eq 1) we find the equations of motion for angles ϕ_i:

$$\ddot{\phi}_i = \sum_{j=1,\, j\neq i}^{N}\frac{\mu_i\mu_j}{I_i r_{ij}^3}\sin(\phi_i - \phi_j) \tag{4}$$

The solution of these equations of motion is the trajectory that describes the time evolution of the dipoles. In case of two altitudinal dipoles the solution can be found analytically, as will be shown in the next section.

In the case of the azimuthal dipole chains, the dipoles are still rotating in the xy plane, but the center-to-center distance vectors $\vec{r}_{ij}$ are pointing in the x direction, $\vec{r}_{ij} = (r_{ij}, 0, 0)$. Hence, the scalar product of $\vec{r}_{ij}$ with the dipole moments is nonzero:

$$L = \sum_{i=1}^{N}\frac{I_i}{2}\dot{\phi}_i^2 - \sum_{i=1}^{N-1}\sum_{j=i+1}^{N}\frac{\mu_i\mu_j}{r_{ij}^3}[\cos(\phi_i - \phi_j) - 3\cos\phi_i\cos\phi_j] \tag{5}$$

The Euler−Lagrange equations give

$$\ddot{\phi}_i = \sum_{j=1,\, j\neq i}^{N} \frac{\mu_i \mu_j}{I_i r_{ij}^3}[\sin(\phi_i - \phi_j) - 3\sin\phi_i \cos\phi_j] \qquad (6)$$

In the case of $N = 2$, with I_1 equal to I_2, eq 6 can be solved analytically.

3. Two-Dipole Systems: Dimers

For a better understanding of the energy transfer in dipole chains, the nature of the interaction between two dipoles must be known. Therefore, we start with an analysis of two-dipole systems (dimers).

Altitudinal Dimer. Applying the Euler−Lagrange equation (eq 1) to eq 3 for two altitudinal dipoles yields equations of motion for the angles ϕ_1 and ϕ_2:

$$I_1\ddot{\phi}_1 = \frac{\mu_1\mu_2}{r_{12}^3}\sin(\phi_1 - \phi_2) \qquad (7)$$

$$I_2\ddot{\phi}_2 = -\frac{\mu_1\mu_2}{r_{12}^3}\sin(\phi_1 - \phi_2) \qquad (8)$$

Adding both equations shows that the total angular momentum $I_1\dot{\phi}_1 + I_2\dot{\phi}_2$ is conserved:

$$I_1\ddot{\phi}_1 + I_2\ddot{\phi}_2 = \frac{\mathrm{d}}{\mathrm{d}t}(I_1\dot{\phi}_1 + I_2\dot{\phi}_2) = 0 \qquad (9)$$

Subtracting eq 8 from eq 7 gives an equation of motion for the difference angle $\phi_{12} = \phi_1 - \phi_2$:

$$\ddot{\phi}_{12} = \omega_0^2 \sin\phi_{12} \qquad (10)$$

where

$$\omega_0^2 = \frac{\mu_1\mu_2}{r_{12}^3}\frac{I_1 + I_2}{I_1 I_2} \qquad (11)$$

In this paper reduced units (see Appendix) are used, $\mu_1 = \mu_2 = I_1 = I_2 = r_{12} = 1$. Equation 10 is almost identical to the equation of motion for the physical pendulum, except for the sign. Transformation $\phi_{12} \rightarrow \phi + \pi$ makes it identical:

$$\ddot{\phi} = -\omega_0^2 \sin\phi \qquad (12)$$

The solution of the physical pendulum is well-known and given by

$$\dot{\phi}(t) = \pm\sqrt{2}\omega_0(\cos\phi(t) + C)^{1/2} \qquad (13)$$

$$\sqrt{2}\omega_0 t = \int_{\phi(0)}^{\phi(t)} (\cos\psi + C)^{-1/2}\mathrm{d}\psi \qquad (14)$$

in which C is an integration constant that depends on the initial conditions $\phi(0)$ and $\dot{\phi}(0)$:

$$C = \frac{1}{2\omega_0^2}\dot{\phi}^2(0) - \cos\phi(0) \qquad (15)$$

In this paper the initial orientations of the dipoles in the systems are such that the systems are in the ground state. For the altitudinal systems this is the case if the dipoles are oriented antiparallel. Hence, $\phi(0) = 0$. Initially all dipoles but the first are at rest. The first dipole is excited, giving it an angular velocity $\dot{\phi}_1(0)$. Hence, $\dot{\phi}(0) = \dot{\phi}_1(0)$.

Depending on the magnitude of the excitation, there are two possibilities: First, if the excitation is such that $C < 1$, then, according to eq 13, $\dot{\phi}(t)$ is zero for

$$\cos\phi_{\max} = -C \qquad (16)$$

and therefore ϕ will oscillate between $-\phi_{\max}$ and $\phi_{\max}$.

Second, if the initial excitation is so high that $C > 1$, then there is no value for $\phi_{\max}$, for which a solution of eq 16 exists, and hence $\phi_{\max}$ does not exist: $\phi(t)$ does not oscillate but increases continuously (the pendulum rotates). Note that if $\dot{\phi}(0) < 0$, then $\phi(t)$ decreases continuously. Figure 2 presents these results graphically (Animations of these results and all other results of this article can be found on webpage http://www.chem.northwestern.edu/~tcgrp/jjdej/articles/MDC3ET.html).

The excitation that marks the boundary between oscillatory and rotational behaviors ($C = 1$) is in this paper called the critical excitation $\dot{\phi}_C$. For identical dipoles $\omega_0^2 = 2$, and eq 15 gives $\dot{\phi}_C = 2\sqrt{2}$ in case of the altitudinal dimer.

The top graphs of Figure 2 present the evolution in time of the two dipoles for two different excitations; a low excitation on the left-hand side $\dot{\phi}(0) = 1.0 < \dot{\phi}_C$, and a high excitation on the right-hand side $\dot{\phi}(0) = 3.0 > \dot{\phi}_C$. Starting from a ground-state configuration implies that the second dipole starts at a value $\phi_2(0) = \pi$. The graphs show for a low excitation that the two dipoles follow each other as they rotate, whereas for a high excitation the excited dipole rotates faster than the second dipole. The trajectories of $\phi(t)$ are in the middle graphs, in which $\phi(t)$ oscillates for the low excitation and increases continuously in time for the high excitation. The sum of the angles obeys the conservation of total angular momentum and increases in both cases linearly with the initial angular velocity.

The bottom graphs show the kinetic energies of the dipoles. The dipoles exchange kinetic energy completely every period for an excitation below $\dot{\phi}_C$, whereas for high excitation only a part of the kinetic energy of the excited dipole is exchanged.

Since transfer of kinetic energy is the main focus of this paper, it is interesting to see when the largest transfer occurs. Conservation of angular momentum yields

$$I_1\dot{\phi}_1(t) + I_2\dot{\phi}_2(t) = I_1\dot{\phi}(0) \qquad (17)$$

and with $\phi(t) = \phi_1(t) - \phi_2(t)$ it is easy to show that

$$\dot{\phi}_2(t) = \frac{I_1}{I_1 + I_2}(\dot{\phi}(0) - \dot{\phi}(t)) \qquad (18)$$

Hence the kinetic energy of the second dipole is

$$E_2^{\mathrm{kin}}(t) = \frac{1}{2}I_2\dot{\phi}_2^2(t) = \frac{I_2}{2}\left(\frac{I_1}{I_1 + I_2}\right)^2(\dot{\phi}(0) - \dot{\phi}(t))^2 \qquad (19)$$

We can now consider the two types of motion.

(1) Oscillatory Motion: $0 \le \dot{\phi}(0) \le 2\omega_0$. Equation 19 shows clearly that E_2^{kin} reaches its maximum when $\dot{\phi}(t)$ reaches its minimum. In this case $\phi(t)$ oscillates between $-\phi_{\max}$ and $\phi_{\max}$ and its derivative $\dot{\phi}(t)$ between $-\dot{\phi}(0)$ and $\dot{\phi}(0)$, hence, the minimum of $\dot{\phi}(t)$ is $-\dot{\phi}(0)$. Then eq 19 becomes, in terms of $\dot{\phi}(0)$ or initial (and maximum) kinetic energy of the first dipole $E_{1,\max}^{\mathrm{kin}}$,

$$E_{2,\max}^{\mathrm{kin}} = 2I_2\left(\frac{I_1}{I_1 + I_2}\right)^2\dot{\phi}^2(0) = 4\frac{I_1 I_2}{(I_1 + I_2)^2}E_{1,\max}^{\mathrm{kin}} \qquad (20)$$

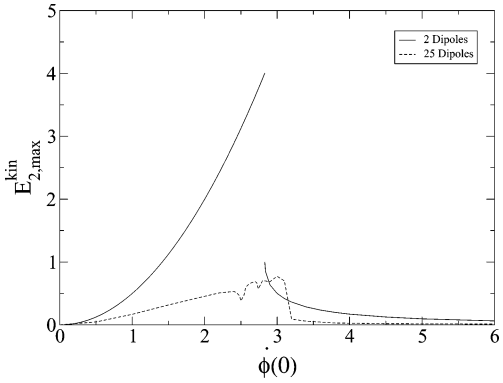

Figure 3. The maximum kinetic energy in the second dipole $E^{kin}_{2,max}$ versus the excitation $\dot{\phi}(0)$ for the altitudinal pair (solid line). There is a maximum value of 4 units for $\dot{\phi}(0) = \dot{\phi}_C = 2\sqrt{2}$. The dashed line shows the maximum kinetic energy the 10th dipole in a 25-dipole chain reaches when the signal passes versus the excitation for the altitudinal chain as a measure of energy transferred through the chain.

The maximum kinetic energy is linear in the excitation energy. Note that the prefactor has a maximum equal to unity for $I_1 = I_2 = I$. In this case the maximum energy transfer is 100%. For $I_1 \neq I_2$ it is always less than 100%.

(2) Rotational Motion: $\dot{\phi}(0) \geq 2\omega_0$. Now, $\dot{\phi}(t)$ is always positive and $\phi(t)$ increases continuously. Equations 13 and 15 show that $\dot{\phi}(t)$ reaches a minimum of

$$\dot{\phi}_{min} = \sqrt{\dot{\phi}_2^0 - 4\omega_0^2} \tag{21}$$

whenever $\phi(t) = (2n + 1)\pi$. Substituting this into eq 19 gives the maximum kinetic energy of the second dipole for high excitations:

$$E^{kin}_{2,max} = I_2\left(\frac{I_1}{I_1 + I_2}\right)^2\left(\dot{\phi}^2(0) - 2\omega_0^2 - \dot{\phi}(0)\sqrt{\dot{\phi}^2(0) - 4\omega_0^2}\right) \tag{22}$$

or, in terms of the initial kinetic energy of the excited dipole $E^{kin}_{1,max}$,

$$E^{kin}_{2,max} = \frac{2I_1I_2}{(I_1 + I_2)^2}\left(E^{kin}_{1,max} - I_1\omega_0^2 - \sqrt{(E^{kin}_{1,max})^2 - 2I_1\omega_0^2\,E^{kin}_{1,max}}\right) \tag{23}$$

For very high excitations, $\dot{\phi}(0) \gg 2\omega_2$, eqs 22 and 23 behave as

$$E^{kin}_{2,max} = I_2\left(\frac{I_1}{I_1 + I_2}\right)^2\frac{4\omega_0^4}{\dot{\phi}^2(0)} = \frac{8I_1I_2}{(I_1 + I_2)^2}\frac{(I_1\omega_0^2)^2}{E^{kin}_{1,max}} \tag{24}$$

The energy transfer decays with the inverse square of the excitation angular velocity $\dot{\phi}(0)$ and with the inverse of the excitation energy $E^{kin}_{1,max}$.

Filling in the critical excitation $\dot{\phi}(0) = 2\omega_0$ and $E^{kin}_{1,max}$ in eq 20 gives a maximum kinetic energy transfer $E^{kin}_{2,max} = 2I\omega_0^2$, whereas eqs 22 and 23 give $E^{kin}_{2,max} = 1/2\ I\omega_0^2$. Figure 3 shows the maximum kinetic energy of the second dipole, $E^{kin}_{2,max}$, as a function of the excitation, $\dot{\phi}(0)$. It is discontinuous in its critical excitation, see Figure 3. One can see that the energy transfer is largest close to, but not higher than, the critical excitation.

Azimuthal Dimer. A similar analysis is made for the azimuthal dimer. Applying the Euler−Lagrange equation (eq 1) to eq 5 results in two equations of motion:

$$I_1\ddot{\phi}_1 = \frac{\mu_1\mu_2}{r_{12}^3}[\sin(\phi_1 - \phi_2) - 3\sin\phi_1\cos\phi_2] \tag{25}$$

$$I_2\ddot{\phi}_2 = \frac{\mu_1\mu_2}{r_{12}^3}[-\sin(\phi_1 - \phi_2) - 3\cos\phi_1\sin\phi_2] \tag{26}$$

Addition of the equations of motion yields

$$I_1\ddot{\phi}_1 + I_2\ddot{\phi}_2 = -3\frac{\mu_1\mu_2}{r_{12}^3}\sin(\phi_1 + \phi_2) \tag{27}$$

which shows that the total angular momentum is **not** conserved in this system. Subtracting eq 26 from eq 25 yields

$$I_1\ddot{\phi}_1 - I_2\ddot{\phi}_2 = -\frac{\mu_1\mu_2}{r_{12}^3}\sin(\phi_1 - \phi_2) \tag{28}$$

Equations 27 and 28 cannot be solved analytically unless the dipoles have the same moment of inertia, $I_1 = I_2 = I$. In this case the system can be described in terms of the difference angle $\phi = \phi_1 - \phi_2$ and the sum of the angles $\Phi = \phi_1 + \phi_2$:

$$\ddot{\phi} = -\omega_1^2\sin\phi \tag{29}$$

$$\ddot{\Phi} = -\omega_2^2\sin\Phi \tag{30}$$

where $\omega_2^2 = 3\omega_1^2 = 3/2\omega_0^2$. Both equations are identical to the physical pendulum. The solutions of the equations are of the same form as eqs 13 and 14, substituting ω_1^2 and ω_2^2 for ω_0^2 for ϕ and Φ, respectively. The terms $\dot{\phi}(t)$ and $\dot{\Phi}(t)$ behave the same way as $\dot{\phi}(t)$ in case of the altitudinal dimer. Hence, both have a (different) critical excitation. Using the ground-state positions ($\phi_1(0) = \phi_2(0) = 0$ and so $\phi(0) = \Phi(0) = 0$) we find their critical excitations: $\dot{\phi}_C = 2\omega_1 = 2$ and $\dot{\Phi}_C = 2\omega_2 = 2\sqrt{3}$.

Since the system has two critical excitations, the excitation domain of $\dot{\phi}(0)$ for the azimuthal dimer can be split in three regions. Note that since the initial angular velocity of the second dipole is zero, both initial angular velocities $\dot{\phi}(0)$ and $\dot{\Phi}(0)$ are equal to $\dot{\phi}_1(0)$. From now on $\dot{\phi}(0)$ will be used as the excitation angular velocity. In the first region, for which $\dot{\phi}(0) < \dot{\phi}_C$, both $\phi(t)$ and $\Phi(t)$ oscillate between their maximum values. In the middle region, for which $\dot{\phi}_C < \dot{\phi}(0) < \dot{\Phi}_C$, the excitation is high enough that $\phi(t)$ is no longer oscillatory, but $\Phi(t)$ still is. In the last region, for which $\dot{\phi}(0) > \dot{\Phi}_C$, $\Phi(t)$ is also no longer oscillatory, i.e., both angles change continuously with time.

Figure 4 shows the system's evolution graphically. There are three series presented corresponding to the three regions of $\dot{\phi}(0)$. The graphs of $\phi(t)$ and $\Phi(t)$ are in agreement with what is described above. The three top graphs show the evolution of the angles of the dipoles ϕ_1 and ϕ_2. In the first region both $\phi_1(t)$ and $\phi_2(t)$ are periodic. In the second region both dipoles rotate with the same (average) speed but in opposite directions. The difference between the angle increases, and the sum of the angles oscillates. In the third region, the second dipole cannot keep up with the excited dipole and rotates more slowly in the opposite direction. Now, both the difference angle and the sum of the angles increase continuously.

The bottom graph presents the kinetic energy of the dipoles. The first two regions show that there is no full periodic transfer of kinetic energy. However, we will show later in this section that the maximum kinetic energy of the second dipole is equal

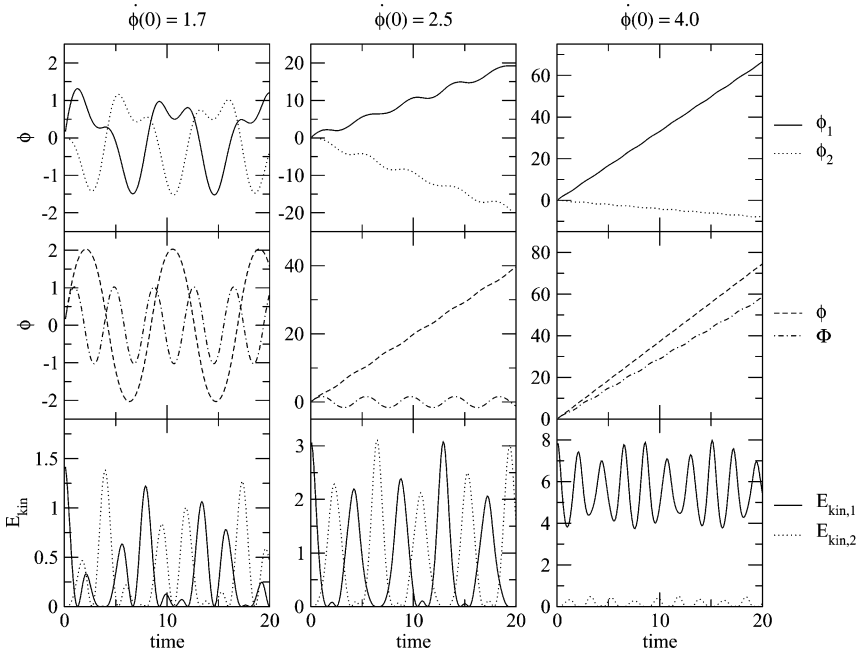

Figure 4. Angles and kinetic energies for an azimuthal dimer system. There are three regions with three different types of behavior.

to that of the first one. The graphs show that for high excitations $\dot{\phi}(0) > \dot{\Phi}_C$ the kinetic energy transfer is very small.

The kinetic energy of the second dipole can be written as

$$E_2^{\text{kin}}(t) = \frac{1}{2} I \dot{\phi}_2^2(t) \tag{31}$$

where

$$\dot{\phi}_2(t) = \frac{1}{2}\left(\dot{\Phi}(t) - \dot{\phi}(t)\right) \tag{32}$$

and the equations for $\dot{\Phi}$ and $\dot{\phi}$ have the same form as eq 13:

$$\dot{\Phi}(t) = \pm\sqrt{2\omega_1^2 \cos\Phi - 2\omega_1^2 + \dot{\phi}^2(0)} \tag{33}$$

$$\dot{\phi}(t) = \pm\sqrt{2\omega_2^2 \cos\phi - 2\omega_2^2 + \dot{\phi}^2(0)} \tag{34}$$

Three separate cases can now be distinguished.

(1) Oscillatory Motion of Both Φ *and* ϕ*:* $0 \le \dot{\phi}(0) \le 2\omega_1$. Oscillatory motion for both dipoles implies that both angular velocities vary between $-\dot{\phi}(0)$ and $\dot{\phi}(0)$. From equations 31 and 32 it follows that the maximum kinetic energy transfer to dipole two occurs whenever the difference between the angular velocities is the largest, i.e., $\dot{\Phi}(t) = -\dot{\phi}(t) = \pm\dot{\phi}(0)$, in which case

$$E_{2,\max}^{\text{kin}} = \frac{1}{2} I \dot{\phi}^2(0) = E_{1,\max}^{\text{kin}} \tag{35}$$

The transfer is then 100%. Such a condition can occur only if the ratio T_Φ/T_ϕ of the periods for Φ and ϕ is a rational number, which is clearly not the case, since

$$\frac{T_\Phi}{T_\phi} = \frac{\omega_1}{\omega_2} = \frac{1}{\sqrt{3}} \tag{36}$$

However, one can always find two integers n and m such that

$$\frac{n}{\left(m + \frac{1}{2}\right)\sqrt{3}}$$

is arbitrarily close to unity, in which the transfer is arbitrarily close to 100%. Hence, one can argue that the energy transfer is 100% in this case.

(2) Rotational Motion for ϕ*, Oscillatory Motion for* Φ*:* $2\omega_1 \le \dot{\phi}(0) \le 2\omega_2$. The rotational motion for ϕ implies that $\dot{\phi}(t)$ is always positive, i.e., $\phi(t)$ increases continuously. The maximum energy transfer occurs when $\dot{\Phi} = -\dot{\phi}(0)$ and $\dot{\phi} = \dot{\phi}(0)$:

$$E_{2,\max}^{\text{kin}} = \frac{1}{2} I \dot{\phi}^2(0) = E_{1,\max}^{\text{kin}} \tag{37}$$

which represents 100% efficiency.

(3) Rotational Motion of Both Φ *and* ϕ*:* $\dot{\phi}(0) \ge 2\omega_2$. In this case $\dot{\Phi}(t)$ and $\dot{\phi}(t)$ are both positive so that $\Phi(t)$ and $\phi(t)$ both increase monotonically with time. Using the positive values of eqs 33 and 34 in eq 32 gives the kinetic energy of the second dipole:

$$E_2^{kin}(t) = \frac{I}{4}\left\{\omega_1^2(\cos\phi - 1) + \omega_2^2(\cos\Phi - 1) + \dot{\phi}^2(0) - 2\sqrt{\left(\omega_1^2(\cos\phi - 1) + \frac{1}{2}\dot{\phi}^2(0)\right)\left(\omega_2^2(\cos\Phi - 1) + \frac{1}{2}\dot{\phi}^2(0)\right)}\right\} \tag{38}$$

or in terms of excitation energy $E_{1,\max}^{\text{kin}}$

$$E_2^{\text{kin}}(t) = \frac{I}{4}\omega_1^2(\cos\phi - 1) + \frac{I}{4}\omega_2^2(\cos\Phi - 1) + \frac{1}{2}E_{1,\max}^{\text{kin}} - \frac{1}{2}\sqrt{(I\omega_1^2(\cos\phi - 1) + E_{1,max}^{kin})(I\omega_2^2(\cos\Phi - 1) + E_{1,max}^{kin})} \tag{39}$$

These are not only functions of the excitation but also of the angles Φ and ϕ. Figure 5 shows the energy transfer as a function of angles ϕ and Φ. (Note that the function is even in Φ and ϕ, so only $0 \le \Phi, \phi \le \pi$ is plotted.) The maximum occurs for cos $\phi = -\cos\Phi = 1$, in which case eqs 38 and 39 become

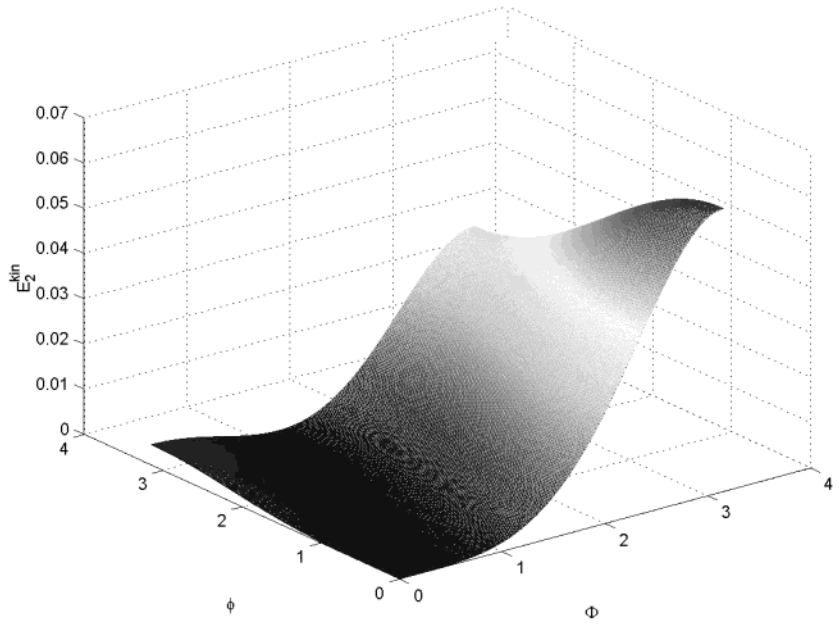

Figure 5. Kinetic energy of the second dipole as a function of the rotation angles ϕ and Φ for an excitation higher that the critical excitation, $\dot{\phi}(0) > \dot{\Phi}_C$.

$$E_{2,\max}^{\text{kin}} = \frac{I}{4}\left(\dot{\phi}^2(0) - 2\omega_2^2 - \sqrt{\dot{\phi}^2(0)(\dot{\phi}^2(0) - 4\omega_2^2)}\right)$$
$$= \frac{1}{2}\left(E_{1,\max}^{\text{kin}} - I\omega_2^2 - \sqrt{E_{1,\max}^{\text{kin}}(E_{1,\max}^{\text{kin}} - 2I\omega_2^2)}\right) \quad (40)$$

For very high excitations these behave as

$$E_{2,\max}^{\text{kin}} = \frac{I\omega_2^4}{2\dot{\phi}^2(0)} = \frac{I^2\omega_2^4}{4E_{1,\max}^{\text{kin}}} \quad (41)$$

The energy transfer is inversely proportional to the excitation energy for high excitations.

Again, a discontinuity is found at the critical excitation $\dot{\phi}(0) = \dot{\Phi}_C = 2\omega_2$. From eq 35 we find a value of $E_{2,\max}^{\text{kin}} = 2I\omega_2^2$, whereas eqs 38 and 39 give $E_{2,\max}^{\text{kin}} = 1/2\ I\omega_2^2$. Figure 6 shows the maximum transferred energy versus the excitation.

Summary. In this section we found that the azimuthal dimer system is described by two angular variables, whereas the altitudinal dimer needs only one due to the conservation of total angular momentum. The three angle variables behave as physical pendula, each showing two types of motion. For low excitations, the angle of the pendulum and its time derivative oscillate between their maxima defined by the initial conditions. For high excitations, the angle increases continuously in time and the derivative is always positive. The altitudinal dimer has only one variable, and therefore two regimes of energy transfer. The azimuthal dimer has two independent variables, resulting in three different regimes of energy transfer.

Regarding the energy transfer, we find a similar excitation dependence for both systems. The transferred energy is linear in the excitation energy up to a certain critical excitation. At higer excitations (Figures 3 and 6), the initially excited dipole retains most of the kinetic energy. A higher critical excitation allows the azimuthal dimer to transfer more energy. The azimuthal dimer transfers at most 6 units of kinetic energy at $\dot{\phi}(0) = 2\omega_2 = 2\sqrt{3}$, whereas the altitudinal dimer transfers at most 4 units at $\dot{\phi}(0) = 2\omega_0 = 2\sqrt{2}$.

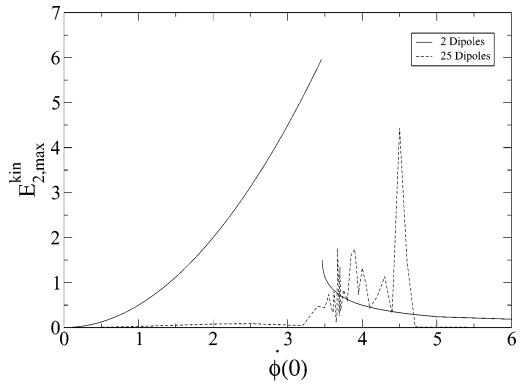

Figure 6. The maximum kinetic energy in the second dipole $E_{2,\max}^{\text{kin}}$ versus the excitation $\dot{\phi}(0)$ for the azimuthal pair (solid line). There is a maximum value of 6 units for $\dot{\phi}(0) = \dot{\phi}_C = 2\sqrt{3}$. The dashed line shows the maximum kinetic energy the 10th dipole in a 25-dipole chain reaches when the signal passes versus the excitation for the azimuthal chain as a measure of energy transferred through the chain.

4. Dipole Chains

We now examine dipole chains containing 25 dipoles. Low energy excitations have been discussed previously.[6−8] For arbitrarily high energy excitations no analytic solutions exist, but numerical solutions are readily attainable by dynamical simulations. We apply the Velocity Verlet algorithm[12] to integrate the equations of motion.

Altitudinal Dipole Chains. Figure 7 shows the time evolution of the angles ϕ_i and kinetic energies E_i^{kin} for selected dipoles in a 25 altitudinal dipole chain with low initial excitation, $\dot{\phi}(0) = 1.0$. Due to the excitation, the first dipole rotates an amount $\phi_{\text{step}} \approx 1.2$ rad (Figure 7, $i = 1$). The rotation is followed by the other dipoles, and travels as a signal through the chain. Figure 8 shows the configuration of the dipole chain after 17 time units. One can see that the first 11 dipoles are rotated by an amount 1.2 rad ≈ 70 deg and the 12th dipole just started its rotation. After ≈32 time units, when all the dipoles have rotated over ϕ_{step}, the signal has reached the last dipole in the chain, where it is reflected back. Then every dipole rotates another ϕ_{step} rad. Every time the signal reaches an end of the chain, it is reflected.

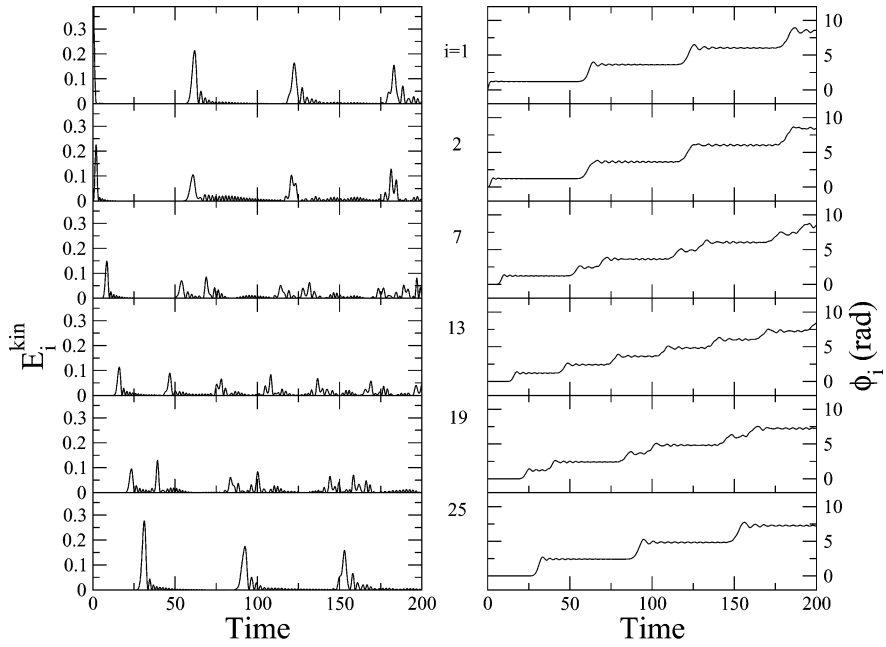

Figure 7. Time evolution of the angles ϕ_i and the kinetic energy E_i^{kin} of a 25 altitudinal dipole chain for a low excitation ($\dot{\phi}(0) = 1.0$). A small but distinguishable soliton-like signal travels through the chain (note that the initial conditions are such that neighboring dipoles are antiparallel: $\phi_i(0) = (-1)^{i\pi/2}$).

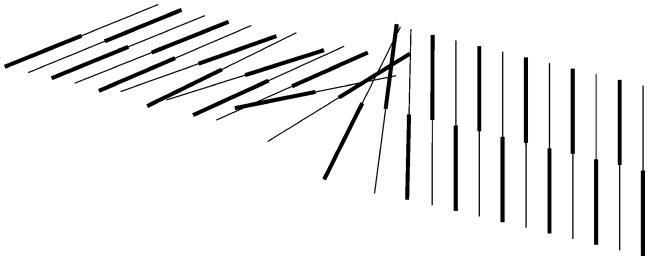

Figure 8. Picture of the 25 dipole altitudinal chain 11 time units after the first dipole was excited $\dot{\phi}(0) = 1.0$. The excitation makes the dipoles rotate one by one over roughly 70 degrees.

The kinetic energy graphs show the soliton-like traveling signal very clearly. The height of the energy pulse decreases as it travels through the chain. From 0.5 energy units at the excited dipole to 0.22 units at the second, and 0.15 at the 7th (Figure 7). The major cause is the disruption of the ground state as the dipoles rotate by an amount ϕ_{step}. Approximately 0.2 energy units are lost immediately to potential energy. As the signal reaches the 25th dipole, the whole chain is rotated by an amount ϕ_{step}, and the potential energy is minimal again. An increase in the kinetic energy pulse height is clearly visible.

Another cause for the loss of kinetic energy is the accumulation of residual energy on the other dipoles. When the kinetic energy of the second dipole reaches its maximum, other dipoles are (still/already) rotating. Figure 9 shows the peak values of the kinetic energy pulses for each of the dipoles in the chain. The exchanges with the potential energy are indicated by the immediate decrease at the beginning of the chain and the increase at the end. The loss due to kinetic energy residues is indicated by the slow decay from the second to the 24th dipole.

For high excitations there is very little energy transfer through the chain. Figure 10 presents the trajectory and the kinetic energies of the dipoles for a high excitation ($\dot{\phi}(0) = 3.4$). The excited dipole is rotating too rapidly for the second dipole and the rest of the chain to follow. It rotates at an almost constant speed, $\approx$3 rad per time unit. Only a small part of the kinetic energy is transferred into the chain, resulting in traveling signal, a rotation over $\phi_{step} \approx 0.45$ rad every 30 time units.

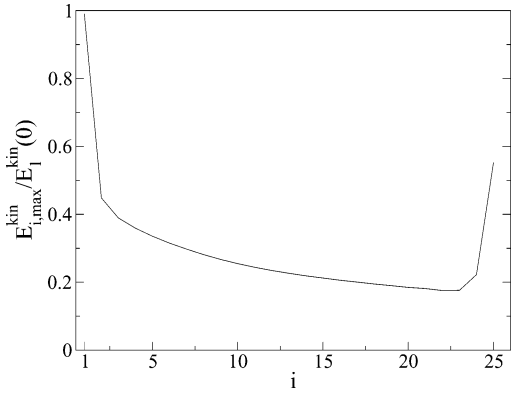

Figure 9. The maximum individual kinetic energy that each dipole reaches as the energy travels through the altitudinal chain, relative to the initial excitation $\dot{\phi}(0) = 1.0$.

How does the system behave between the regions of low and high excitation behavior, i.e., how does the transition from low to high excitation behavior occur? Figure 3 presents the maximum kinetic energy of the 10th dipole (as a measure of transferred energy) versus the excitation. For low excitations ($\dot{\phi}(0) < 2.4$) the transferred energy increases essentially linearly with the excitation, and for high excitations ($\dot{\phi}(0) > 3.2$) there is very little signal transfer. The transition from low excitation behavior to high excitation behavior ($2.4 < \dot{\phi}(0) < 3.2$) is not smooth. There are dips in the graph, of which the largest occurs at $\dot{\phi}(0) = 2.5$. These dips are caused by the following. The higher the excitation, the harder it is for the second dipole to follow the excited dipole. At some point the rotation speed of the excited first dipole is so high that it makes a full rotation (or more) before transfer occurs. The dips in the graph appear just before this point where the second dipole maximally lags the excited dipole. Transfer now takes a long time, and this results in a broader energy pulse, which is therefore lower in amplitude. At $\dot{\phi}(0) = 2.8$ there is a second smaller dip, which is the point just before the excited dipole makes two full rotations before transfer. At $\dot{\phi}(0) = 3.0$, 25 rotations are required for maximal transfer and for excitations higher than 3.2, the

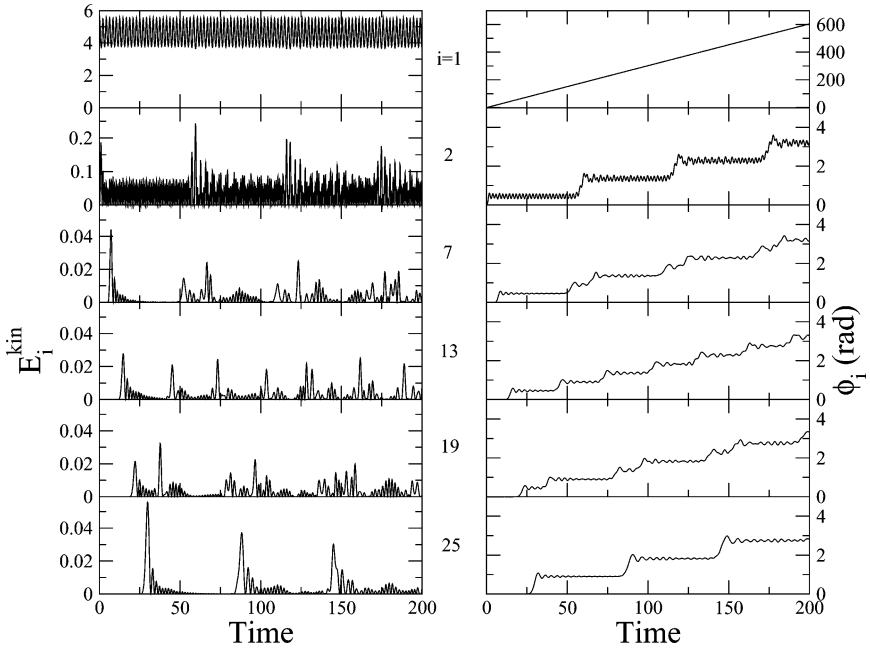

Figure 10. Trajectory of a 25 altitudinal dipole chain for a high excitation ($\dot{\phi}(0) = 3.4$). There is almost no energy transfer in the chain.

second dipole never catches up and the system is in its high excitation behavior.

The graphs in Figure 3 resemble each other in shape. Extending the dimer system to a multidipole system has little influence on the excitation domain in which energy transfer occurs. Where the energy transfer is complete for the dimer, we find a lower amount of transferred energy in the chain. Nevertheless, the energy transfer behavior of the chain (Figure 3) implies a device application: The chain of altitudinal dipoles responds essentially linearly to low excitations but produces no output for high excitations, i.e., it behaves like a high excitation filter.

As described in ref 8 the antiferromagnetic altitudinal chain exhibits some interesting behavior in the case that the 50th dipole in a chain of 100 dipoles is excited with a kinetic energy of 10 units ($\dot{\phi}(0) = 4.47$). It was found that initially a small amount of energy leaks to its nearest neighbors, and a more profound and explicit secondary energy transfer occurs after approximately 75 time units (see Figure (13)). Roughly 2 units of kinetic energy are transferred to the neighboring dipoles.

Comparing these results with the previous section, we see that the primary energy transfer behaves as expected. It is very small since the excitation is above the critical value of $\dot{\phi}(0) = 3.2$. However, in our calculations the secondary energy transfer does not occur. The secondary transfer in the chain that is excited in the middle finds its origin in the potential energy. The excited dipole rotates so rapidly that there is no net interaction with the neighboring dipoles. Initially the 49th and 51st are parallel to each other because of the ground-state initial positions. After the 50th dipole is excited, the neighboring dipoles prefer an antiparallel orientation: they realign resulting in a $\pi/2$ and $-\pi/2$ phase change for each chain end, respectively. If, instead of the middle dipole, the first dipole in the chain is excited, only one neighboring dipole exists, and no phase change is induced. Hence, no secondary energy transfer occurs.

Azimuthal Dipole Chains. Low excitations result in no (noticeable) energy transfer in a 25 azimuthal dipole chain. The trajectories in Figure 12 ($\dot{\phi}(0) = 1.0$) show that the excited dipole oscillates with a large amplitude (0.6 rad); this amplitude is attenuated by about half at the second dipole, and in the rest of the chain there is little motion. From the graphs of the kinetic energies one sees that only a very small part of the energy travels through the chain. The 7th dipole reaches a maximum kinetic energy that is 6% of the excitation energy, and less than 4% reaches the end of the chain. Most of the excitation energy remains on the initially excited dipole as kinetic and potential energy.

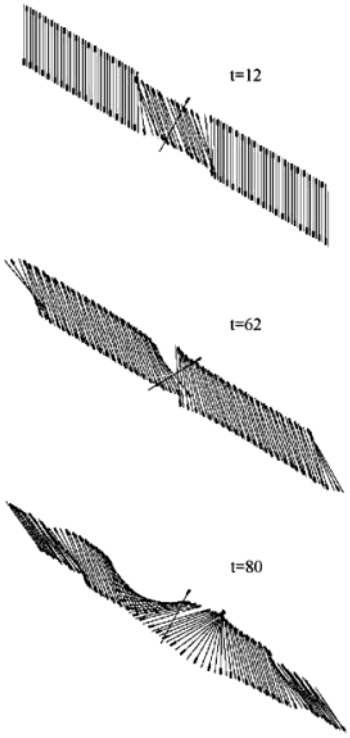

Figure 11. Configuration pictures of the 100 dipole altitudinal chain that is excited at the 50th dipole $\dot{\phi}(0) = 4.47$. The first picture shows the chain configuration shortly after the excitation ($t = 12$). Note that the dipoles directly neighboring the excited dipole are parallel. The middle picture shows the configuration while the secondary energy transfer is occurring ($t = 62$); the neighboring dipoles start their phase change of $\pi/2$ and $-\pi/2$, respectively. The bottom figure shows the configuration after the secondary energy transfer ($t = 80$). The dipoles directly neighboring the excited dipole have finshed their phase change and are now antiparallel.

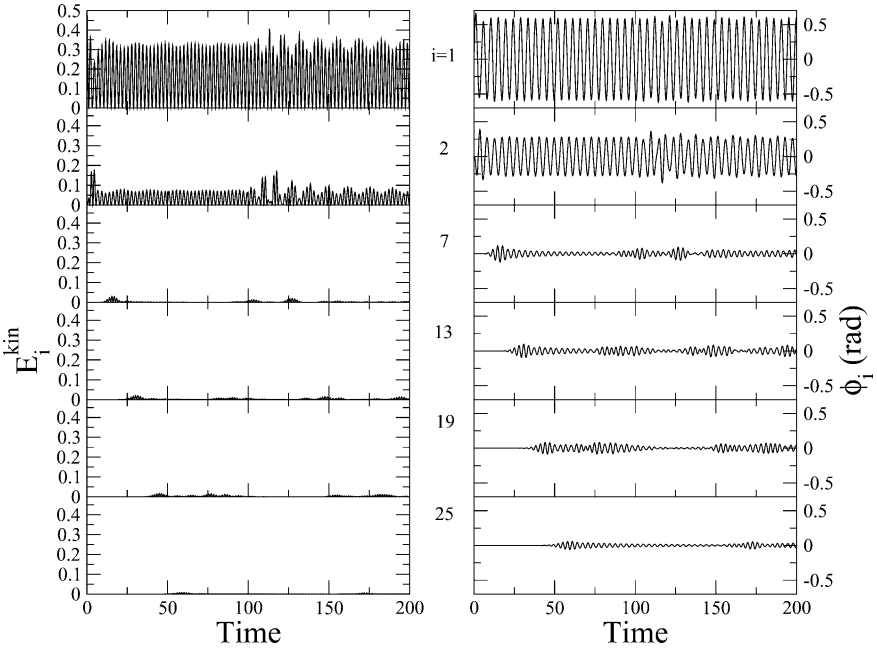

Figure 12. Trajectory of a 25 azimuthal dipole chain for a low excitation ($\dot{\phi}(0) = 1.0$). The excitation does not lead to a soliton-like transfer in the chain. Most of the energy remains on the excited dipole.

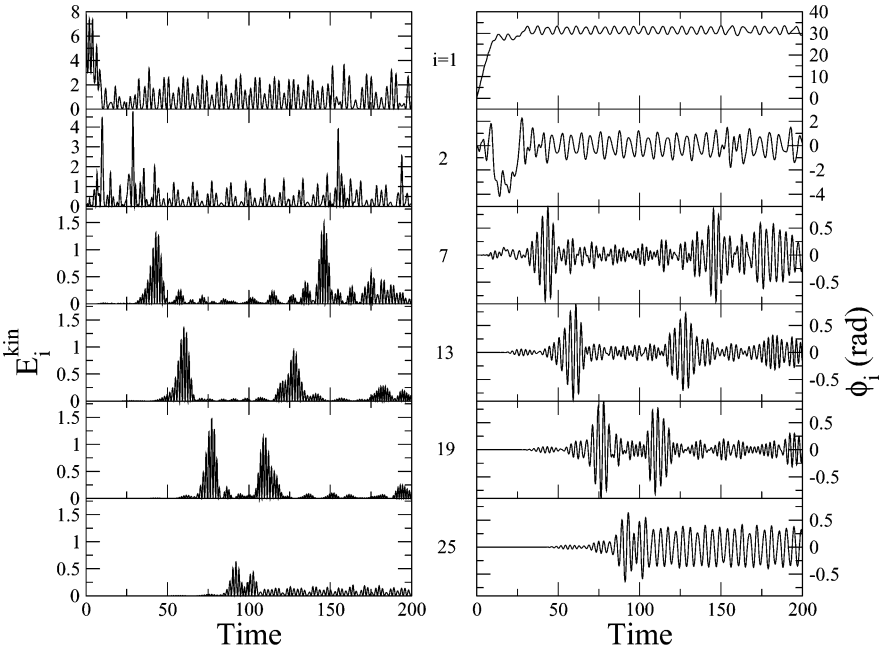

Figure 13. Trajectory of a 25 azimuthal dipole chain for an excitation that results in a packet-like signal transfer ($\dot{\phi}(0) = 4.0$).

For high excitations the behavior resembles the high excitation behavior of the altitudinal dipole chain: The excited dipole rotates too rapidly for the rest of the chain to follow, and as for low excitations ($\dot{\phi}(0) = 1.0$) in the azimuthal chain, only a small amount of energy is transferred to the rest of the chain.

Figure 6 shows the maximum kinetic energy of the 10th dipole versus the excitation as a measure of the transferred energy. The transition from low ($\dot{\phi}(0) < 3.2$) to high ($\dot{\phi}(0) > 4.7$) excitation behavior is more erratic than for the altitudinal dipole chain. Small changes in the excitation lead to a completely different behavior. It is obvious that for certain excitations energy is transferred through the chain. Figure 13 shows the trajectory for the $\dot{\phi}(0) = 4.0$ excitation (near a peak in Figure 6); here a packet-like behavior is visible both in the trajectory and in the kinetic energy graph. However, for other excitations there is no such behavior and the excitation energy is spread over the dipoles in the chain. The propensity for energy transfer is determined by both the excitation and the initial configuration.

The excitation dependence of the azimuthal dipole chain is different from that of the dimer (compare the graphs in Figure 6). Where the dimer responds to low excitations and not to high excitations (a high excitation filter), the chain acts more as a band filter: only certain excitations between $3.2 < \dot{\phi}(0) < 4.7$ result in a packet-like energy transfer. In this paper all quantities are in reduced units, and their corresponding real values change for different dipole molecules and the interrotor distance (see Appendix). A device that detects certain excitations can be designed varying these features of the dipole chain.

Summary. Comparing the two dipole chains, we find that both chains act similarly for high excitations. The excited dipole rotates too rapidly and the rest of the chain cannot follow its

motion. Most of the excitation energy stays at the excited dipole, and only a small amount is transferred to the rest of the chain.

For low excitations the altitudinal dipole chain shows a soliton-like energy transfer through the chain. The amount of transferred energy increases with the excitation. If the excitation is too high ($\dot{\phi}(0) > 2.4$) the rest of the chain can no longer efficiently follow the excited dipole's motion. Above a critical point it cannot follow the motion at all and the chain goes into its high excitation behavior regime ($\dot{\phi}(0) > 3.2$).

The azimuthal dipole chain shows effectively no energy transfer for low excitations. Most of the energy remains on the excited dipole. For some excitations in the transition region ($3.2 < \dot{\phi}(0) < 4.7$) we find a soliton-like energy transfer in the chain, but for most excitations a small portion of the energy spreads over the dipoles in the chain in a wider distribution.

The energy transfer graphs (3,6) indicate possibilities for device applications. The altitudinal chain responds linearly to the excitation until a certain cutoff excitation, whereas the azimuthal chain acts as a crude band filter.

5. Concluding Remarks

We calculated the trajectories for initially excited azimuthal and altitudinal one-dimensional dipole chains, varying the excitation in an attempt to find soliton-like energy propagation in these chains. To have a better understanding of the interaction between dipoles, two-dipole systems (dimers) were investigated first.

For the dimers the energy transfer from the initially excited dipole to the other one is linear in the excitation energy up to a certain value $\dot{\phi}_C$. At higher $\dot{\phi}$ the excited dipole rotates too rapidly for the second to follow its motion. Since the critical excitation energy is higher for the azimuthal dimer than for the altitudinal dimer, more energy is transferred within the azimuthal dimer.

Trajectory calculations of the chains show limited soliton-like energy transfer for both chain types. At low excitation energies, energy transfer within the altitudinal chain varies almost linearly with initial excitation energy. However, for high initial excitation no energy transfer occurs. The altitudinal dipole chain behaves as a high excitation filter. Also, if the chain is excited not at the end but in the middle, a secondary, more unusual energy transfer occurs. It is caused by the realignment of the two chain segments.

In case of the azimuthal dipole chain, we found that a soliton-like energy transfer occurs only for certain excitation energies. Small changes in initial excitation lead to energy dissipation in the chain that is not soliton-like. For both low and high initial excitation there is no noticeable energy transfer in the chain.

So far we have explored totally perfect one-dimensional dipole chains. More interesting behavior of these chains can be found if different initial conditions are used, or friction and temperature are added in the model.[11] Future research will also include an investigation of two-dimensional systems, such as branching and crossing chains.

Acknowledgment. We are grateful to Josef Michl, Jaroslav Vacek, Alex Burin, and Neil Snider for their helpful remarks. This work was funded by the ARO through the DURINT program.

Appendix: Reduced Units

Reduced units were used in derivations of analytical solutions and in MD calculations. All units can be calculated from their corresponding reduced units (in this appendix noted with *) if three variables are known: the dipole moment, μ_0, and the moment of inertia, I_0, of the dipole rotor, and the distance between the rotors, r_0.

$$\vec{\mu} = \mu_0 \cdot \vec{\mu}^* \tag{42}$$

$$I = I_0 \cdot I^* \tag{43}$$

$$\vec{r} = r_0 \cdot \vec{r}^* \tag{44}$$

Properties of the system that are calculated in reduced units now can be converted into real units. Reduced energy E^* becomes real energy E using

$$E = \frac{\mu_0^2}{4\pi\epsilon_0 r_0^3} \cdot E^* \text{ [J]} \tag{45}$$

Similarly, time t and excitation angular velocity $\dot{\phi}(0)$ can be found from their reduced units:

$$t = \sqrt{\frac{4\pi\epsilon_0 I_0 r_0^3}{\mu_0^2}} \cdot t^* \text{ [s]} \tag{46}$$

$$\dot{\phi}(0) = \sqrt{\frac{\mu_0^2}{4\pi\epsilon_0 I_0 r_0^3}} \cdot \dot{\phi}(0)^* \text{ [rad/s]} \tag{47}$$

Applying these equations on a chain of dipole rotors with dipole moments $\mu_0 = 2D$, and moments of inertia $I_0 = 114$ amuÅ^2 and a nearest neighbor interrotor distance $r_0 = 15$ Å, we find that every reduced energy unit corresponds to 0.017 kcal/mol, each time unit corresponds with 0.266 ps, and each excitation unit to 600 rotations per ns.

References and Notes

(1) Hersam, M. C.; Lee, J.; Guisinger, N. P.; Lyding, J. W. *Superlatt. Microstruct.* **2000**, *27*(5−6), 583.

(2) Hale, P. D.; Ratner M. A. *J. Chem. Phys* **1985**, *83*, 5277. Hale, P. D.; Pietro, W. J.; Ratner, M. A.; Ellis, D. E.; Marks, T. J. *J. Am. Chem. Soc.* **1987**, *109*, 5943. Bohm, M. C.; Staib, A. *J. Phys. Chem.* **1992**, *96*(8), 3465.

(3) Van de Craats, A. M.; Siebbeles, L. D. A.; Bleyl, I.; Haarer, D.; Berlin, Y. A.; Zharikov, A. A.; Warman, J. A.; *J. Phys. Chem. B* **1998**, *102*, 9625.

(4) Jimenez-Ruiz, M.; Criado, A.; Bermejo, F. J. *J. Phys. Condens. Mater.* **2002**, *14(7)*, 1509.

(5) Ogawa, M. Y.; Martinsen, J.; Palmer, S. M.; Stanton, J. L.; Tanaka, J.; Greene, R. L.; Hoffman, B. M.; Ibers, J. A.; *J. Am. Chem. Soc.* **1985**, *109*, 1115.

(6) Rozenbaum, V. M. *Phys. Rev. B* **1995**, *51*, 1290. Rozenbaum, V. M.; Lin, S. H. *J. Chem. Phys.* **2000**, *112*, 9083.

(7) de Leeuw, S. W.; Solvaeson, D.; Ratner, M. A.; Michl, J. *J. Phys. Chem. B* **1998**, *102*, 3876.

(8) Sim, E.; Ratner; M. A.; de Leeuw, S. W. *J. Phys. Chem. B* **1999**, *103*, 8663.

(9) Rozenbaum V. M. *Phys. Rev. B* **1995**, *53*, 6240. Rozenbaum, V. M. *JETP Lett.* **1996**, *63*, 662. Rozenbaum, V. M. *Phys. Solid State* **1998**, *40*, 136.

(10) Haldane, F. D. M. *J. Phys. A* **1982**, *15*(2), 507.

(11) Clarke, L. I.; Horinek, D.; Kottas, G. S.; Varaksa, N.; Magnera, T. F.; Hinderer, T. P.; Horansky, R. D.; Michl, J.; Price, J. C. *Nanotechnology* **2002**, *13*, 533.

(12) For example, see Thijssen, J. M. *Computational Physics*; Cambridge University Press: Cambridge, 1999.